British Journal of Pharmacology (2008) 153, 367–379

0007–1188/08 $30.00
www.brjpharmacol.org

RESEARCH PAPER

Differential effects of cannabinoid receptor agonists on regional brain activity using pharmacological MRI

C-L Chin[1], AE Tovcimak[1], VP Hradil[1], TR Seifert[1], PR Hollingsworth[2], P Chandran[2], CZ Zhu[2], D Gauvin[2], M Pai[2], J Wetter[3], GC Hsieh[2], P Honore[2], JM Frost[2], MJ Dart[2], MD Meyer[2], BB Yao[2], BF Cox[1] and GB Fox[1]

[1]*Advanced Technology, Global Pharmaceutical Research and Development, Abbott Laboratories, Abbott Park, IL, USA;* [2]*Neurological Diseases Research, Global Pharmaceutical Research and Development, Abbott Laboratories, Abbott Park, IL, USA and* [3]*Exploratory Kinetics & Analysis, Global Pharmaceutical Research and Development, Abbott Laboratories, Abbott Park, IL, USA*

Background and purpose: Activation of cannabinoid CB_1 and/or CB_2 receptors mediates analgesic effects across a broad spectrum of preclinical pain models. Selective activation of CB_2 receptors may produce analgesia without the undesirable psychotropic side effects associated with modulation of CB_1 receptors. To address selectivity *in vivo*, we describe non-invasive, non-ionizing, functional data that distinguish CB_1 from CB_2 receptor neural activity using pharmacological MRI (phMRI) in awake rats.
Experimental approach: Using a high field (7 T) MRI scanner, we examined and quantified the effects of non-selective CB_1/CB_2 (A-834735) and selective CB_2 (AM1241) agonists on neural activity in awake rats. Pharmacological specificity was determined using selective CB_1 (rimonabant) or CB_2 (AM630) antagonists. Behavioural studies, plasma and brain exposures were used as benchmarks for activity *in vivo*.
Key results: The non-selective CB_1/CB_2 agonist produced a dose-related, region-specific activation of brain structures that agrees well with published autoradiographic CB_1 receptor density binding maps. Pretreatment with a CB_1 antagonist but not with a CB_2 antagonist, abolished these activation patterns, suggesting an effect mediated by CB_1 receptors alone. In contrast, no significant changes in brain activity were found with relevant doses of the CB_2 selective agonist.
Conclusion and implications: These results provide the first clear evidence for quantifying *in vivo* functional selectivity between CB_1 and CB_2 receptors using phMRI. Further, as the presence of CB_2 receptors in the brain remains controversial, our data suggest that if CB_2 receptors are expressed, they are not functional under normal physiological conditions.
British Journal of Pharmacology (2008) **153,** 367–379; doi:10.1038/sj.bjp.0707506; published online 29 October 2007

Keywords: cannabinoid; CB_1; CB_2; AM1241; A-834735; phMRI; fMRI; awake rat

Abbreviations: A-834735, 1-(tetrahydro-pyran-4-ylmethyl)-1H-indol-3-yl]-(2,2,3,3-tetramethyl-cyclopropyl)-methanone; AM1241, 2-iodo-5-nitrophenyl-[1-(1-methylpiperidin-2-yl-methyl)-1H-indol-3-yl-methanone]; AM630, (6-iodo-2-methyl-1-(2-morpholin-4-yl-ethyl)-1H-indol-3-yl)-(4-methoxy-phenyl)-methanone; CB_1, cannabinoid 1; CB_2, cannabinoid 2; PAG, periaqueductal grey; phMRI, pharmacological magnetic resonance imaging; rCBV, relative cerebral blood volume; rimonabant (SR1, SR141716A), 5-(4-chloro-phenyl)-1-(2,4-dichloro-phenyl)-4-methyl-1H-pyrazole-3-carboxylic acid piperidin-1-ylamide

Introduction

The pharmacological effects of cannabis and its derivatives, collectively known as cannabinoids, are mediated via two known G-protein-coupled receptor subtypes: cannabinoid 1 (CB_1) receptors that are found predominantly in the central nervous system (CNS); and CB_2 receptors that are expressed by immune cells in the periphery and whose presence in the CNS remains controversial (Croxford, 2003; Pertwee, 2006). Although analgesic properties of cannabinoids have been known for many years (Richardson *et al.*, 1998; Iversen and Chapman, 2002), the therapeutic use of cannabinoid ligands is severely limited by CB_1-mediated cognitive, motor and psychotropic side effects (Campbell *et al.*, 2001; Mackie,

Correspondence: Dr GB Fox, Experimental Imaging/Advanced Technology, Global Pharmaceutical Research and Development, Abbott Laboratories, R46R, AP9-1, 100 Abbott Park Road, Abbott Park, IL 60064, USA.
E-mail: gerard.b.fox@abbott.com
Received 3 July 2007; revised 23 August 2007; accepted 18 September 2007; published online 29 October 2007

2006). This has created an opportunity to investigate selective CB_2 receptor agonists as a novel class of potential analgesic drugs (Malan *et al*., 2003). Indeed, it has recently become apparent that selective activation of CB_2 receptors in rodents inhibits acute nociceptive, hyperalgesic (Malan *et al*., 1998), inflammatory (Gutierrez *et al*., 2007) and chronic pain (Ibrahim *et al*., 2003), confirming broad-spectrum efficacy. Unfortunately, there are no reliable and unambiguous methods available to predict *in vivo* functional selectivity for CB_2 vs CB_1 receptors.

Pharmacological magnetic resonance imaging (phMRI) is an *in vivo* neuroimaging technique that offers high spatial and temporal resolution in animals and humans and is being increasingly exploited to map regional changes in neural activity following pharmacological challenges (Leslie and James, 2000; Honey and Bullmore, 2004; Fox *et al*., 2006; Wise and Tracey, 2006). In preclinical studies, a number of neurotransmitter systems have been investigated using phMRI, including dopaminergic (Chen *et al*., 1997; Schwarz *et al*., 2004; Dixon *et al*., 2005; Ireland *et al*., 2005), GABAergic (Reese *et al*., 2000; Xi *et al*., 2002), nicotinic (Gozzi *et al*., 2005; Choi *et al*., 2006; Skoubis *et al*., 2006; Chin *et al*., 2007) and glutamatergic (Jones *et al*., 2005) systems. Notably, in many of these preclinical studies, anaesthesia was used to immobilize animals to alleviate motion artefacts. However, anaesthesia is rarely used in clinical phMRI studies since it is known to dampen basal neuronal activity and can potentially obscure observed activation patterns (Austin *et al*., 2005; Chin *et al*., 2007). Consequently, there is growing interest in imaging awake animals including rodents and monkeys (Zhang *et al*., 2000; Fox *et al*., 2006; Skoubis *et al*., 2006).

In this study, we sought to differentiate CB_1 from CB_2 receptor-mediated changes in neural activity, a reflection of *in vivo* functional selectivity at these receptor subtypes and thus a means of determining liability associated with CB_1 activation. We achieved this by the systemic administration of a non-selective CB_1/CB_2 receptor agonist, 1-(tetrahydropyran-4-ylmethyl)-1H-indol-3-yl]-(2,2,3,3-tetramethyl-cyclopropyl)-methanone (A-834735), or the CB_2 receptor-selective agonist, 2-iodo-5-nitrophenyl-[1-(1-methylpiperidin-2-yl-methyl)-1H-indol-3-yl-methanone] (AM1241) during relative cerebral blood volume (rCBV)-based phMRI data acquisition (Chen *et al*., 1997; Mandeville *et al*., 1998) in awake rats. In addition, to demonstrate pharmacological specificity, blockade studies were also conducted in rats pretreated with the CB_1 receptor antagonist, 5-(4-chloro-phenyl)-1-(2,4-dichlorophenyl)-4-methyl-1H-pyrazole-3-carboxylic acid piperidin-1-ylamide (rimonabant) or the CB_2 receptor antagonist, 6-iodo-2-methyl-1-(2-morpholin-4-yl-ethyl)-1H-indol-3-yl)-(4-methoxy-phenyl)-methanone (AM630). Group average phMRI activation maps were calculated for each treatment group, and spatial-temporal dynamics of drug-induced changes in brain activity were quantified using region of interest (ROI) analyses from several brain structures. Imaging data were then compared to *in vitro* binding and functional data as well as *in vivo* behavioural data using exposure levels as a benchmark. We demonstrate that functional selectivity for CB_2 vs CB_1 receptors can be readily assessed and quantified *in vivo* using non-invasive phMRI in awake rats.

Methods

Animals

Adult male Sprague–Dawley naive rats (Charles River, Portage, MI, USA) were used for all imaging ($n=56$; 300–350 g), pharmacokinetic ($n=12$; 300–350 g) and *in vivo* characterization ($n=116$; 250–350 g) experiments. Rats were group-housed in temperature-controlled (22°–24 °C) rooms and maintained on a 12 h/12 h light/dark cycle with lights on at 0600 hours. Rat chow and water were provided *ad libitum*. All studies were conducted in accordance with Institutional Animal Care and Use Committee (IACUC) guidelines at Abbott Laboratories as well as the National Institutes of Health Guide for Care and Use of Laboratory Animals guidelines. Facilities at Abbott Laboratories are further accredited by the Association for the Assessment and Accreditation of Laboratory Animal Care (AAALAC).

In vivo *imaging*

Animal preparation. To minimize stress during awake imaging (King *et al*., 2006), rats were habituated to a dedicated animal holder identical to the one used for imaging (Insight Neuroimaging Systems, Worcester, MA, USA), receiving four training sessions of varying lengths (7, 30, 60, 60 min, on four separate days) prior to imaging. Additionally, to mimic the environment inside the magnet bore during imaging, acclimitization was carried out inside a ventilated acoustic chamber where a tape-recording of the noise generated by imaging gradients was played. Prior to training, rats were anaesthetized with ~3% isoflurane for positioning inside the holder and then allowed to recover from anaesthesia during the habituation period. On the day of imaging, rats were again briefly anaesthetized with isoflurane (5% induction, 3% maintenance in air), placed into the imaging holder. A 24-gauge intravenous catheter (BD Insyte, Becton Dickinson, Franklin Lakes, NJ, USA) was used for lateral tail vein cannulation and was subsequently connected to PE190 tubing via a rotating adaptor (Cole-Parmer Instrument Co., Vernon Hills, IL, USA) for infusion of contrast agent and drugs. Rats were allowed to recover from the effects of isoflurane within the imaging holder in the magnet for approximately 20 min before imaging.

Drug preparation and administration. A-834735 (Dart *et al*., 2006), AM1241, AM630 and rimonabant (SR141716A) were dissolved in PEG 400 or 5% dimethyl sulphoxide/PEG400. Rats were divided into different treatment groups and administered i.v. with: vehicle ($n=6$), A-834735 at 0.3, 1 or 3 $\mu mol\,kg^{-1}$ (0.1, 0.3, 1 $mg\,kg^{-1}$) ($n=5$ per dose), AM1241 at 30 $\mu mol\,kg^{-1}$ (16 $mg\,kg^{-1}$) or 100 $\mu mol\,kg^{-1}$ (54 $mg\,kg^{-1}$) ($n=5$ per dose), AM630 6 $\mu mol\,kg^{-1}$ (3 $mg\,kg^{-1}$) ($n=5$) or rimonabant at 13 $\mu mol\,kg^{-1}$ (6 $mg\,kg^{-1}$) ($n=5$). All compounds were administered at physiological pH in an injection volume of 1 $ml\,kg^{-1}$ at an infusion rate of 0.16 $ml\,min^{-1}$. For antagonist blockade experiments, rats were pretreated with either rimonabant 13 $\mu mol\,kg^{-1}$, i.p. ($n=5$) or AM630 6 $\mu mol\,kg^{-1}$, i.p. ($n=5$) approximately 40 min before the infusion of A-834735 1 $\mu mol\,kg^{-1}$ i.v. In a separate experiment, AM1241 30 $\mu mol\,kg^{-1}$ i.p. ($n=5$) was

also used as a pretreatment to determine whether this compound exhibited any functional antagonist activity when given 40 min prior to i.v. administration of 1 μmol kg^{-1} A-834735.

Pharmacological MRI. All experiments were conducted on a 7 T Bruker Biospec MRI scanner (Karlsruhe, Germany). For both anatomical and functional data, a fast spin-echo pulse sequence was used to image awake rats with imaging parameters: TR/TE$_{eff}$ = 3200/70 ms, rare factor = 16, in-plane resolution = 300 × 300 μm^2, slice thickness = 1.5 mm, two averages. There were 13 contiguous slices prescribed in the coronal plane, centred to cover the majority of the brain including the cerebellum. To improve phMRI sensitivity, an ultrasmall superparamagnetic iron oxide contrast agent with a long blood half-life (Tombach *et al*., 2004) was administered i.v. at a dose of 15 mg Fe kg^{-1}. Experiments were carried out based on the following imaging protocols: (i) 4 min baseline acquisition (pre-contrast agent); (ii) bolus injection of the contrast agent (infusion rate = 2.5 ml min^{-1} i.v.) via the tail vein; (iii) 15 min pre-drug baseline acquisition; (iv) infusion of either vehicle or drug over a 5 min time interval (infusion rate = 0.16 ml min^{-1} i.v.); and (v) 25 min period of post-drug imaging acquisition.

Imaging data analysis. The AFNI software package (Cox, 1996) and in-house IDL (Research Systems Inc., Boulder, CO, USA) programmes were used for data analysis. To identify activated pixels, cross-correlation coefficients between the time-course raw data and a step function (OFF/ON≡pre-drug baseline/post-drug period) were calculated on a pixel-by-pixel basis within the brain parenchyma region for individual animals. The cross-correlation analysis included a linear baseline to account for the elimination of the contrast agent from the blood. Subsequent *z*-scores were derived from the calculated cross-correlation coefficients. To generate group average phMRI maps for each treatment group, anatomical images obtained from each animal were coregistered onto a template image set by rigid-body translations and rotations; these calculated transformation matrix parameters were then applied to the individual *z*-score maps. Group statistical maps were obtained by averaging the coregistered *z*-score maps retrieved from individual animals with a threshold of $z > 2.58$ ($P < 0.01$, uncorrected), and finally a cluster analysis (cluster size = 16 pixels) was applied to negate isolated pixels. Clusters smaller than 16 3-D connected pixels were not considered active.

To retrieve regional drug-induced rCBV change for each pixel, time-course rCBV change, ΔrCBV(t), was calculated from raw data using the known relationship (Mandeville *et al*., 1998),

$$\Delta rCBV(t) = \ln [S(t)/S_0(t)]/ \ln [S_0(t)/S_{PRE}], \qquad (1)$$

where $S(t)$ is the signal intensity after the drug infusion, $S_0(t)$ is the baseline signal before the drug injection, and S_{PRE} is the mean signal intensity before the administration of contrast agent. After deriving the maps of rCBV change, ROI analyses were performed using regions outlined manually according to a rat brain atlas (Paxinos and Watson, 1998), in which regional mean rCBV changes were retrieved from various cortical and subcortical structures for each treatment group (mean ± s.e. mean). Treatment effects were determined in each ROI by a one-way ANOVA (with Bonferroni correction) followed by a Tukey's test for *post hoc* comparisons, with differences considered statistically significant at $P < 0.05$. Since animals were imaged under awake conditions, MR images can sometimes be susceptible to motion-related artifacts. Subjects were excluded from data analysis *a priori*, if significant ghosting imaging artefacts (>10% of time-course data points) were observed or if head position deviated significantly due to the misplaced/unsecured ear bars. In the current studies, we excluded six rats due to motion artefact, resulting in a 90% (56/62) success rate.

Exposure levels and pharmacokinetic analysis. To evaluate exposure levels at time of maximum drug-induced rCBV change, a satellite pharmacokinetic study was performed. A total of 12 rats were divided into four different treatment groups ($n = 3$ per group): A-834735 1 μmol kg^{-1}, rimonabant 13 μmol kg^{-1}, AM630 6 μmol kg^{-1} and AM1241 30 μmol kg^{-1}. Briefly, animals were anaesthetized with isoflurane and cannulated with a tail vein line for drug administration. To mimic the phMRI study, experiments were carried out following the imaging protocol, as described above. During the time periods of pre-contrast and pre-drug baseline acquisition, rats were kept inside the imaging holder (but outside the magnet on the benchtop in an enclosed area) under awake conditions. Approximately 10 min after drug infusion, rats were re-anaesthetized and removed from the imaging holder. Blood samples were collected via cardiac puncture and brains were then immediately removed and snap-frozen for later analysis. Samples were analysed in our Exploratory Kinetics and Analysis Department. Briefly, compounds were selectively removed from plasma or brain homogenate using liquid–liquid extraction with a mixture of ethyl acetate and hexane (1:1, by volume) at neutral pH. The samples were vortexed vigorously followed by centrifugation. The organic layer was transferred and evaporated to dryness with a gentle stream of nitrogen over low heat (~35 °C). The samples were reconstituted by vortexing with mobile phase. Compounds and their internal standards were separated from co-extracted contaminants on a 50 × 3 × 5 μm Luna CN column with an acetonitrile/0.1% trifluoroacetic acid (50:50, by volume) mobile phase at a flow rate of 0.4 ml min^{-1} with a 25 μl injection. Compounds were quantified using MRM detection with a turbo ionspray source on a mass spectrometer (PE Sciex Applied Biosystems, Foster City, CA, USA). The limits of quantification were approximately 10, 25, 20 and 30 ng ml^{-1} for plasma and 50, 25, 20 and 150 ng g^{-1} for brain samples for A-834735, rimonabant, AM630 and AM1241, respectively.

In vitro *characterization*

Cell culture. Human embryonic kidney (HEK, American Type Culture Collection, Rockville, MD, USA) cells stably expressing rat CB_2 or rat CB_1 receptors were grown in Dulbecco's modified Eagle medium containing high glucose supplemented with 10% foetal bovine serum and 25 μg ml^{-1} zeocin in a 37 °C incubator in the presence of 5% CO_2.

Radioligand binding assay. Membrane samples prepared from HEK cells stably expressing rat CB_2 or rat CB_1 receptors were used to perform radioligand competition binding assays as described previously (Mukherjee *et al*., 2004). Briefly, experiments were conducted using 0.5 nM [^{3}H]CP 55,940 in the presence of variable concentrations of test compounds in an assay buffer containing 2.5 mM EDTA, 5 mM $MgCl_2$, 50 mM Tris–HCl, pH 7.4, and 0.05% fatty acid-free BSA. Reactions were terminated by rapid vacuum filtration through UniFilter-96 GF/C filter plates after 90 min incubation at 30 °C and four washes with cold assay buffer. Nonspecific binding was defined by 10 μM unlabelled CP 55940 and K_i values from competition binding assays were determined with one-site competition curve fitting using Prism (GraphPad, San Diego, CA, USA). HEK cells were used since, although we have demonstrated CB_1 receptor binding using membranes prepared from rat cortex, we were not able to show CB_2 binding using the same membrane preparations.

Cyclase functional assays. The HitHunter cAMP assay kit was used in suspension forms as described previously (Yao *et al*., 2006). Briefly, cell suspensions were incubated at 37 °C for 20 min with variable concentrations of test ligands or 10 μM CP 55,940 positive control in the presence of a fixed concentration of forskolin (18 μM for rat CB_2 line; 37 μM for rat CB_1 line) in Dulbecco's phosphate buffered saline (D-PBS) buffer supplemented with BSA (0.01% final concentration). Reactions were terminated by the addition of lysis buffer and luminescence was detected as per the vendor's directions. The positive control, CP 55940, at a concentration of 10 μM produced significant levels of inhibition on forskolin-induced cAMP levels in rat CB_1 (90% inhibition, $n=10$) and rat CB_2 (63% inhibition, $n=10$) receptor systems, and is used to define 100% efficacy at CB_1 and CB_2 receptors in cyclase assays, respectively. Efficacy of ligands is expressed as percentage response compared to that of 10 μM CP 55940, with agonists in positive and inverse agonists in negative numbers. EC_{50} values were calculated from sigmoid dose response curve fitting using Prism (GradPad Software Inc.).

In vivo *characterization*

Locomotor activity and rotarod assay. To benchmark imaging data against potential CNS side effects of A-834735 using traditional *in vivo* behaviour assays, rotarod performance and spontaneous exploratory behaviour were assessed in naive rats. Briefly, rotorod performance was measured using an accelerating rotorod apparatus (Omnitech Electronics Inc. Columbus, OH, USA). A total of 28 rats ($n=7$ per treatment group) were allowed a 30 min acclimatization period in the testing room and then placed on a 9 cm diameter rod that was set to increase in speed from 0 to 20 r.p.m. over a 60 s period. The time required for the rat to fall from the rod was recorded, with a maximum score of 60 s. Each rat was given three training sessions and then rotorod performance (mean latency to fall from the rotorod) was determined 30 min following i.p. administration of vehicle or A-834735 (0.5, 1.5 or 5 μmol kg^{-1}). For spontaneous exploratory behaviour, a total of 40 rats ($n=8$ per group) were injected i.p. with vehicle (5% dimethyl sulphoxide/PEG400) or A-834735 (0.5, 1.5, 5 and 15 μmol kg^{-1}) in a volume of 2 ml kg^{-1} and returned to their home cages. After 30 min, rats were individually placed into test chambers equipped with an automated photobeam detector system (AccuScan Instruments, Columbus, OH, USA) and exploratory behaviour was recorded as photobeam breaks for a further 30 min. Results for both tests were subjected to a one-way ANOVA followed by *post hoc* comparisons using Fisher's protected least significance difference (PLSD) test, with differences considered statistically significant at $P<0.05$.

Chronic inflammatory and neuropathic pain models. Chronic inflammatory thermal hyperalgesia was induced in a total of 24 rats ($n=6$ per treatment group) by injection of a 50% solution of complete Freund's adjuvant (CFA) in phosphate-buffered saline (volume 150 μl) into the plantar surface of the right hind paw. Thermal hyperalgesia was determined 48 h post-CFA injection using a commercially available thermal paw stimulator (UARDG, University of California, San Diego, CA, USA) as described previously (Hargreaves *et al*., 1988). Rats were placed into individual plastic cubicles mounted on a glass surface maintained at 30 °C, and allowed a 20 min habituation period. A thermal stimulus, in the form of radiant heat emitted from a focused projection bulb, was then applied to the plantar surface of each hind paw. The stimulus current was maintained at 4.50 ± 0.05 A, and the maximum time of exposure was set at 20.48 s to limit possible tissue damage. The elapsed time until a brisk withdrawal of the hind paw from the thermal stimulus was recorded automatically using photodiode motion sensors. The right and left hind paw of each rat was tested in three sequential trials at approximately 5 min intervals. Paw withdrawal latency (PWL) was calculated as the mean of the two shortest latencies. Behavioural testing occurred 30 min following i.p. administration of vehicle or A-834735 (0.1, 0.3 or 1 μmol kg^{-1}).

Spinal nerve ligation-induced neuropathic pain was produced in a total of 24 rats ($n=6$ per treatment group) using the procedure originally described by Kim and Chung (1992). The left L5 and L6 spinal nerves were isolated adjacent to the vertebral column and tightly ligated with a 5-0 silk suture distal to the dorsal root ganglion (DRG), and care was taken to avoid injury of the L4 spinal nerve. All animals were allowed to recover for at least 1 week prior to assessment of tactile allodynia. Tactile allodynia was measured using calibrated von Frey filaments (Stoelting, Wood Dale, IL, USA) as described previously (Chaplan *et al*., 1994). Rats were placed into inverted individual plastic containers on top of a suspended wire mesh grid, and acclimatized to the test chambers for 20 min. The von Frey filaments were presented perpendicularly to the plantar surface of the selected hind paw, and then held in this position for approximately 8 s with enough force to cause a slight bend of the filament. Positive responses included an abrupt withdrawal of the hind paw from the stimulus, or flinching behaviour immediately following removal of the stimulus. A 50% withdrawal threshold was determined using an up–down procedure. Only rats with a baseline threshold score of less that 4.5 g were utilized for pharmacological studies, and

animals demonstrating a motor deficit were excluded. Vehicle or A-834735 (0.1, 0.3 or 1 μmol kg^{-1}) was administered i.p. 30 min prior to testing with von Frey filaments.

Materials

A-834735 (Dart *et al*., 2006), AM1241, AM630 and rimonabant (SR141716A) were synthesized at Abbott Laboratories (Abbott Park, IL, USA) and dissolved in PEG400 (Sigma-Aldrich, St Louis, MO, USA) or 5% dimethyl sulphoxide/PEG400. Ultrasmall superparamagnetic iron oxide contrast agent (SH U 555 C) was obtained from Schering AG (Berlin, Germany) and isoflurane from Abbott Laboratories (Abbott Park). All reagents used for cell culture were purchased from Invitrogen (Carlsbad, CA, USA) unless otherwise indicated. UniFilter-96 GF/C filter plates were from Perkin Elmer (Boston, MA, USA) and HitHunter cAMP assay kit from DiscoveRx (Fremont, CA, USA). D-PBS buffer was purchased from Invitrogen (Carlsbad, CA, USA).

Results

In vivo *imaging*

Effects of A-834735 and AM1241 on phMRI brain activity. A total of 56 awake rats were used for the phMRI investigation of CB_1 and CB_2 receptor activation. The CB_1/CB_2 non-selective agonist, A-834735 produced a dose-related and region-specific change in brain activity patterns that was statistically significant across various brain regions (Figure 1, Table 1). The greatest increases in rCBV, the measure that reflects this increased brain activity, were observed in cortical regions such as the cingulate, motor, prefrontal and somatosensory cortices. Additional brain regions affected included the hippocampus, periaqueductal grey (PAG), nucleus accumbens and striatum. In contrast, no significant changes in brain activation were observed in samples from rats treated with vehicle or with 30 or 100 μmol kg^{-1}of the CB_2-selective agonist, AM1241 (shown for 30 μmol kg^{-1} in Figure 1), despite reaching relatively high brain levels 10 min after dosing in satellite rats treated in a similar manner (Table 2).

Effects of rimonabant and AM-630 on phMRI brain activity. CB_1- (rimonabant) and CB_2- (AM630) selective antagonists were used to determine specificity of observed effects with A-834735. Rats treated in the magnet with antagonists alone (rimonabant 13 μmol kg^{-1} or AM630 6 μmol kg^{-1}) did not display significant changes in brain activity (Figures 2a and c). However, pretreatment with rimonabant abolished the effects of 1 μmol kg^{-1} A-834735, indicating a CB_1 receptor-related mechanism (Figure 2b). In contrast,

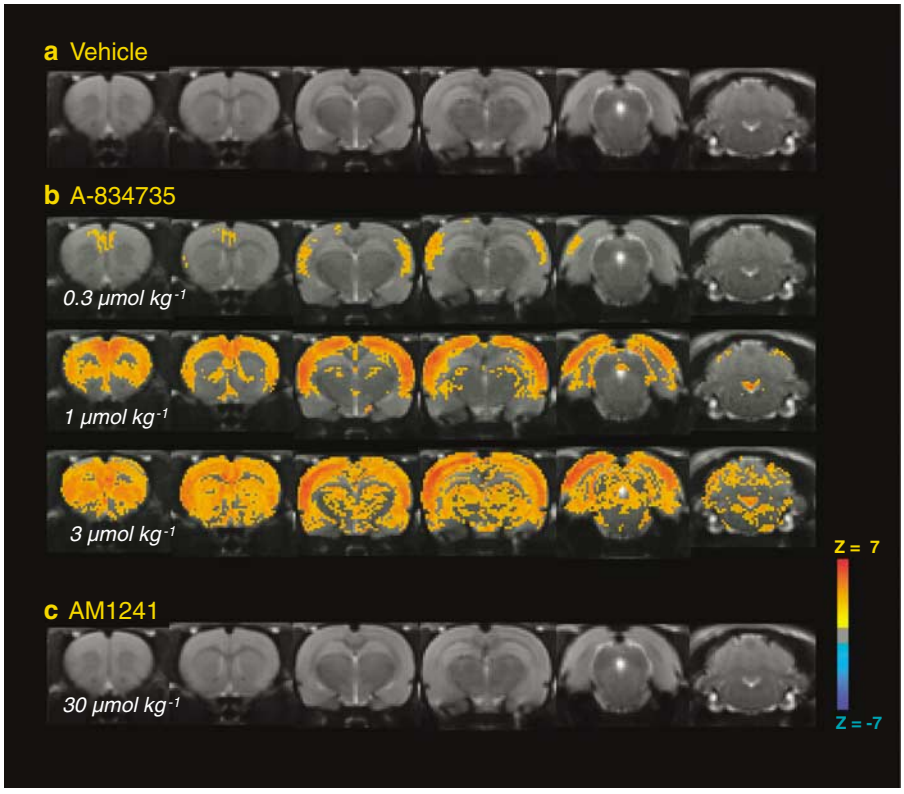

Figure 1 Group average phMRI activation maps (*z*-score; threshold: $z > 2.58$, $P < 0.01$) obtained from awake rats following acute i.v. administration of (**a**) vehicle (PEG400, $n = 6$), (**b**) A-834735 at 0.3, 1 or 3 μmol kg^{-1} ($n = 5$ per dose), or (**c**) AM1241 30 μmol kg^{-1} ($n = 5$). No significant activation was found from rats treated with vehicle (**a**) or AM1241 (**c**). In contrast, A-834735 elicited dose-related, region-specific increases in brain activation in awake rats. At the lowest dose, A-834735 affected only prefrontal, cingulate, motor and somatosensory cortices, whereas the nucleus accumbens, striatum, hippocampus, PAG and cerebellum were activated at higher doses. Data are shown for 6 of 13 slices for clarity. PAG, periaqueductal grey; phMRI, pharmacological magnetic resonance imaging.

Table 1 Regional average percentage rCBV change induced by vehicle or A-834735 in awake rats

Brain region	*rCBV change (%)*			
	Vehicle	*A-834735*		
		0.3 μmol kg^{-1}	*1 μmol kg^{-1}*	*3 μmol kg^{-1}*
Prefrontal cortex	0.5 ± 1.4	18.9.0 ± 6.0*	40.6 ± 0.8**	50.5 ± 7.0**
Cingulate cortex	−0.8 ± 1.2	27.8 ± 9.3*	59.1 ± 5.4**	68.8 ± 13.4**
Motor cortex	0.3 ± 0.8	17.9 ± 7.4*	38.1 ± 3.2**	56.6 ± 14.0**
Nucleus accumbens	0.1 ± 1.0	9.0 ± 3.6	29.6 ± 5.0**	37.5 ± 7.0**
Striatum	0.1 ± 0.7	8.3 ± 3.6	17.5 ± 3.0**	30.0 ± 7.4**
Somatosensory cortex	0.3 ± 0.8	28.7 ± 6.4*	58.3 ± 4.9**	67.8 ± 18.9**
Hippocampus	0.1 ± 1.0	10.5 ± 3.4	22.9 ± 3.6**	28.1 ± 3.8**
Periaqueductal gray	0.5 ± 1.4	11.3 ± 5.1	26.9 ± 4.6**	47.7 ± 9.7**
Cerebellum	−0.1 ± 1.2	11.1 ± 7.2	23.9 ± 3.3**	33.5 ± 6.4**

rCBV, relative cerebral blood volume.
Mean ± s.e. mean, % rCBV change.
*$P<0.05$, **$P<0.01$ vs vehicle.

Table 2 *In vitro* binding and functional selectivity (Sel) data and *in vivo* exposure levels for selected compounds

Compound	*Radioligand binding assay*			*cAMP functional assay*				*Drug level 10-min post-dosing*		
	rCB$_1$	*rCB$_2$*	*rCB$_2$*	*rCB$_1$*		*rCB$_2$*		*Dose (imol kg^{-1}) i.v.*	*Plasma (nM)*	*Brain (nM)*
	K$_i$ *(nM)*	K*i (nM)*	*Sel*	*EC$_{50}$ (nM)*	*Max (%)*	*EC$_{50}$ (nM)*	*Max (%)*			
A-834735	4.6	0.31	15	12	92	0.21	93	1	137	1473
rimonabant	2.8	127	1/41	32	−61	>3k	NA	13	949	2968
AM630	588	6.0	98	>25 k	NA	10	−121	6	199	901
AM1241	115	3.9	30	1970	81	>3k	NA	30	1039	1767

pretreatment with AM630 only partially blocked changes in brain activity induced by 1 μmol kg^{-1} A-834735, particularly in globus pallidus and hippocampal regions (Figure 2d). This may reflect some antagonist activity at CB_1 receptors at the dose used since relatively high brain levels of AM630 were achieved 10 min after dosing in satellite rats treated in a similar manner (Table 2). To determine whether AM1241 could behave as a functional antagonist at CB_1 receptors *in vivo*, we pretreated a separate group of rats with 30 μmol kg^{-1} AM1241 and challenged awake rats in the magnet with 1 μmol kg^{-1} A-834735. Under these conditions, AM1241 did not display any functional antagonism at CB_1 receptors *in vivo* (Figure 3). Using ROI analysis, we quantified percentage change in rCBV for A-834735 with and without pretreatment with rimonabant or AM630 (Figure 4). These findings clearly show that the increased activation induced by A-834735 is mediated by CB_1, but not CB_2, receptors. Time-course imaging data also reveal dose-related increases in brain activity following administration of A-834735. The magnitude and duration of these effects were region-dependent (Figure 5).

In vitro *characterization*

Comparison to ligand affinities and in vitro *functional activity.* *In vitro* radioligand binding and cAMP functional data as well as *in vivo* exposure levels are shown for A-834735, rimonabant, AM630 and AM1241 in Table 2. Doses of A-834735 that produce CB_1-mediated changes in brain activity detected by phMRI produce sufficient brain concentrations to bind CB_1 and CB_2 receptors and induce a functional effect, as predicted by *in vitro* K_i and EC_{50} data in binding and cAMP assays, respectively. Similarly, rimonabant and AM630 achieve sufficient concentrations in the brain to block CB_1 and CB_2 receptors, respectively. Interestingly, despite AM1241 reaching high concentrations in the brain sufficient to affect CB_2 and CB_1 receptor function (Table 2), no change in brain activity was observed with AM1241 (Figure 1).

In vivo *characterization*

Comparison to in vivo *behavioural efficacy and side-effect models.* A total of 116 naive animals were used to determine an *in vivo* efficacy and adverse effects profile for A-834735 to benchmark against phMRI findings. CFA injection into the hind paw induced a significant decrease in PWL to thermal stimulation 48 h following CFA injection (PWL control: 9.7 ± 0.2 s vs PWL inflamed: 5.2 ± 0.1 s, $P<0.01$), demonstrating the development of thermal hyperalgesia (Figure 6a). A-834735 reversed CFA-induced thermal hyperalgesia reaching a 57 ± 3% effect at 1 μmol kg^{-1}, i.p. ($P<0.01$ vs vehicle, Figure 6a). Under the same conditions, A-834735 had no effect on PWL of the contralateral non-inflamed paw compared to vehicle controls, indicative of a specific antihyperalgesic effect in this model and a lack of non-specific confounding effects such as anaesthesia.

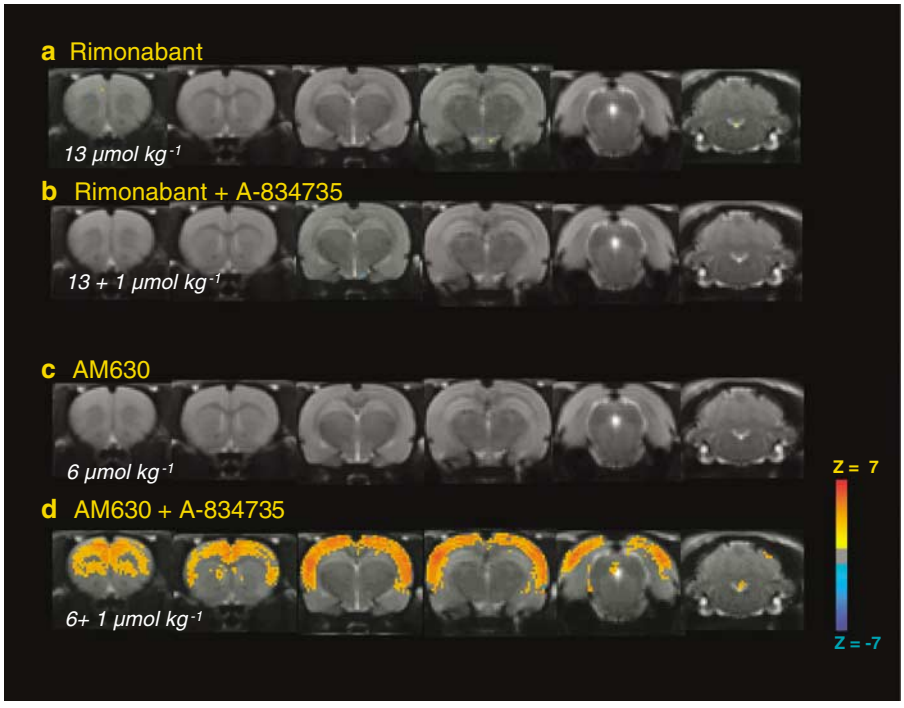

Figure 2 Results of selective antagonist blockade experiments. Group average phMRI activation maps (*z*-score; threshold: $z>2.58$, $P<0.01$) obtained from awake rats treated with (**a**) rimonabant 13 μmol kg^{-1}i.v. ($n=5$), (**b**) pretreatment with rimonabant 13 μmol kg^{-1}i.p., ~40 min prior to infusing A-834735 1 μmol kg^{-1}i.v. ($n=5$ per dose), (**c**) AM630 6 μmol kg^{-1}i.v. ($n=5$) and (**d**) pretreatment with AM630 6 μmol kg^{-1}i.p., ~40 min prior to infusing A-834735 1 μmol kg^{-1}i.v. ($n=5$ per dose). Our data show that rats pretreated with rimonabant, but not with AM630, abolished the effects of 1 μmol kg^{-1} A-834735, indicating a CB_1 mechanism. CB_1, cannabinoid 1; phMRI, pharmacological magnetic resonance imaging.

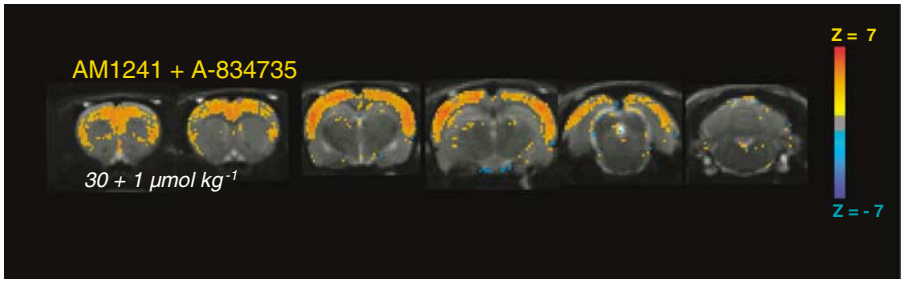

Figure 3 Group average phMRI activation maps (*z*-score; threshold: $z>2.58$, $P<0.01$) obtained from awake rats pretreated with AM1241 30 μmol kg^{-1} i.p., ~40 min prior to infusing A-834735 1 μmol kg^{-1}i.v. ($n=5$). Activation patterns were similar to those obtained from rats infused with A-834735 1 μmol kg^{-1}i.v. ($n=5$, Figure 1b), indicating that AM1241 did not function as a CB_1 antagonist *in vivo* under these conditions. CB_1, cannabinoid 1; phMRI, pharmacological magnetic resonance imaging.

Spinal nerve injury (L5-L6 spinal nerve ligation; Chung model) induced a decrease in paw withdrawal threshold ($PWT_{vonfrey}$) to mechanical stimulation with von Frey monofilaments 2 weeks following injury ($PWT_{vonfrey}$ control 13.3 ± 0.3 g, $PWT_{vonfrey}$ injured 1.7 ± 0.2 g, $P<0.01$) demonstrating the development of mechanical allodynia (Figure 6b). A-834735 reversed spinal nerve injury-induced mechanical allodynia reaching a 76 ± 10% effect at 1 μmol kg^{-1}, i.p. ($P<0.01$ vs vehicle, Figure 6b).

A-834735 did not produce significant locomotor side effects at analgesic doses. However, significant motor side effects were observed; 5 μmol kg^{-1}, i.p., produced a 55 ± 8% decrease in rotorod performance ($P<0.01$ vs vehicle, Figure 7a) and a 40 ± 12% decrease in spontaneous locomotor activity (Figure 7b; nonsignificant vs vehicle). The effects on locomotor activity were more pronounced at 15 μmol kg^{-1} (82 ± 12% effect, $P<0.01$ vs vehicle, Figure 7b).

Discussion and Conclusions

Pharmacological MRI is a relatively new and powerful technique that allows mapping of region-specific changes in brain activation in response to a pharmacological challenge, with high spatial and temporal resolution. We applied a highly sensitive rCBV-based method (Mandeville *et al*., 1998) in naive awake rats (Fox *et al*., 2006) to detect changes in brain activity patterns induced by acute challenge with cannabinoid agonists. Systemic administration of the non-selective CB_1/CB_2 agonist, A-834735, elicited a

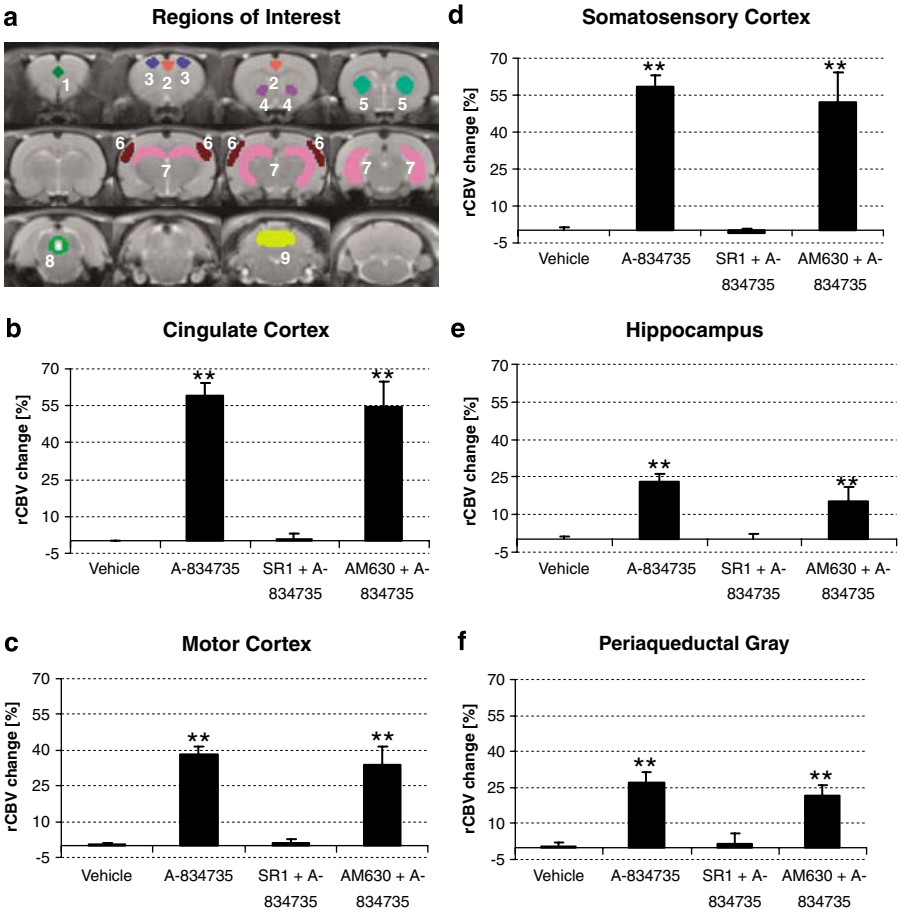

Figure 4 Quantitative ROI analysis of rCBV changes obtained from vehicle, A-834735 1 μmol kg^{-1}, and antagonist blockade (rimonabant or AM630) treatment groups. (**a**) Anatomical images indicating the ROIs analysed: 1-prefrontal cortex, 2-cingulate cortex, 3-motor cortex, 4-nucleus accumbens, 5-striatum, 6-somatosensory cortex, 7-hippocampus, 8-PAG, 9-cerebellum. (**b–f**) Regional mean rCBV changes calculated from cingulate cortex, motor cortex, somatosensory cortex, hippocampus and PAG, respectively. The data show that increases in rCBV induced by A-834735 are abolished by the pretreatment with rimonabant, but not by AM630 (data shown are means ± s.e. mean; $^{**}P<0.01$, vs the vehicle group). PAG, periaqueductal grey; ROI, region of interest; rCBV, relative cerebral blood volume.

region-specific, dose-related activation of cortical and subcortical structures. These effects were specific to activation of CB_1 receptors since they were completely abolished by pretreatment with the CB_1-selective antagonist, rimonabant. In contrast, pretreatment with the CB_2-selective antagonist, AM630, only partially blocked effects of A-834735, consistent with the finding that at high concentrations, AM630 can exhibit antagonist properties at the CB_1 receptor. This observation is informative for *in vivo* studies in general using AM630 as a selective CB_2 receptor antagonist and suggests that investigators should choose their dose carefully to avoid antagonist activity at CB_1 receptors. No changes in brain activity were observed in response to administration of the CB_2-selective agonist, AM1241, indicating that CB_2 receptors, if they are present in the naive rat brain, do not produce a functional response that is detectable using phMRI.

Changes in regional brain activity induced by A-834735 using phMRI in the current studies agree broadly with previously published autoradiography data (Herkenham *et al*., 1990). Using the non-selective, radiolabelled synthetic cannabinoid, [^{3}H]CP 55,940, Herkenham *et al*. (1990) demonstrated that cannabinoid receptors are distributed widely and heterogeneously throughout the brain with high levels of specific binding in basal ganglia and its outflow nuclei, the globus pallidus and substantia nigra, hippocampus and cerebellum. The cerebral cortex also exhibited high levels of binding, especially in the cingulate cortex; of note, the brainstem and thalamus showed relatively low-binding density for [^{3}H]CP 55,940. Similarly, our current data show that rats treated with A-834735 exhibited robust activation in cerebral cortex (particularly the cingulate, prefrontal, motor and somatosensory cortices), striatum, nucleus acumbens, PAG and substantia nigra. Smaller changes in brain activity were observed in the cerebellum, global pallidus, hippocampus and thalamus. Very recently, a positron emission tomography (PET) study in monkey and human brain revealed high uptake of [^{18}F]MK-9470, a selective CB_1 inverse agonist, in brain regions including cerebral cortex and caudate/putamen and relatively low uptake in the hippocampus, pallidum, substantia nigra and cerebellum (Burns *et al*., 2007). Qualitatively, our observed phMRI brain activation patterns agree well with receptor occupancy images obtained from these PET studies. The relatively low functional activity observed using phMRI and

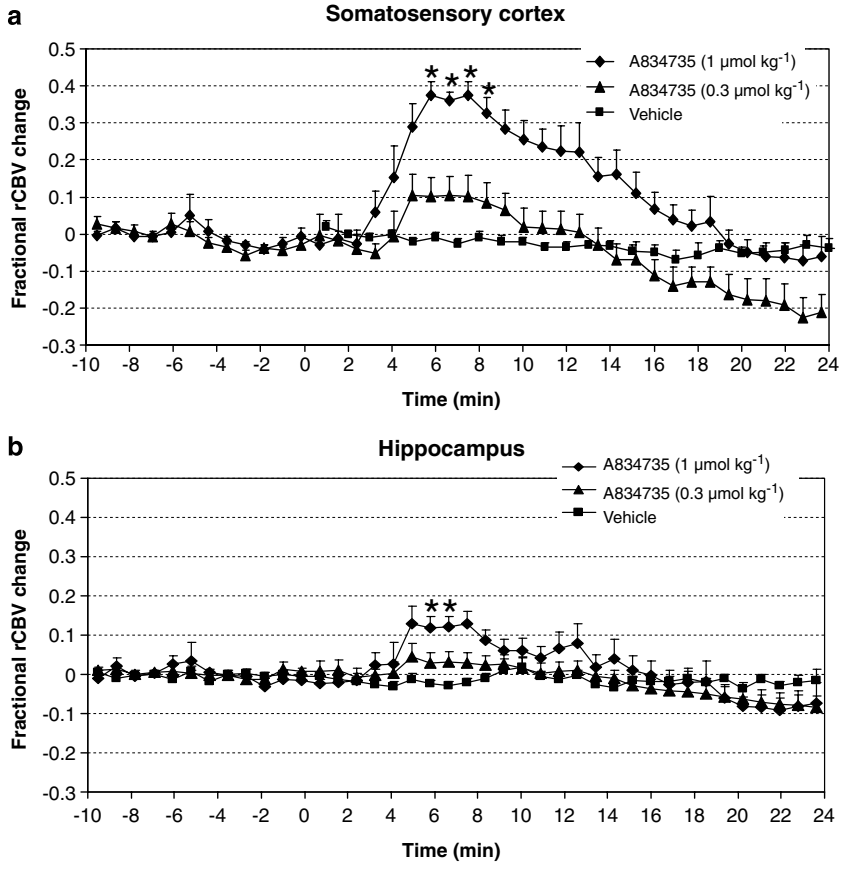

Figure 5 Regional temporal response of A-834735-induced rCBV changes (means ± s.e. mean, $n = 5$ per region) from (**a**) somatosensory cortex and (**b**) hippocampus. For both brain regions, the rCBV temporal response varied in a dose-related manner. The drug was infused from $t = 0$ over a period of 5 min. Interestingly, compared to hippocampus, the onset and magnitude of rCBV changes in somatosensory cortex were earlier and greater, respectively. rCBV, relative cerebral blood volume.

PET in some regions with high CB_1 receptor expression may result from a 'volume effect' since functional *in vivo* imaging studies typically require averaging over a relatively 'thick' virtual slice (in the current phMRI studies with A-834735, we used a slice thickness of 1.5 mm) compared with thin sections used in autoradiography. This is an observation also made by the authors of the recent PET study (Burns *et al*., 2007). However, it is also possible that differences between phMRI maps and autoradiographic receptor binding data in specific brain regions may result from weak neurovascular coupling locally (that is, poor coupling between CB_1 receptors and their effectors in these regions), or that the observed rCBV changes may result from possible downstream effects, instead of direct action at the local site. Another potential explanation could be that the behavioural state of the rats during awake imaging precludes some neurons from being active, and thus there would be no activity for CB_1 receptor stimulation to inhibit. Regardless of the reasons, it is important to note that while it is satisfying to observe a good overlap between autoradiography and phMRI, these techniques measure quite different aspects of receptor pharmacology and do not have to match identically. Our results differ from those of a previous study describing changes in blood oxygenation level-dependent phMRI following administration of the non-selective cannabinoid agonist (HU210), in which relatively large blood oxygenation level-dependent signal changes (~2.5%) were observed in superior colliculus, dorsal PAG and lateral posterior hypothalamus (Shah *et al*., 2004). However, the findings of Shah *et al*. (2004) also differ from the recent PET and earlier autoradiographic data described above. These differences may reflect the low sensitivity of the system employed in the HU210 study (blood oxygenation level-dependent technique in a low field in anaesthetized rats).

While CB_1 receptors are highly expressed in the CNS and cannabinoids acting at presynaptic CB_1 receptors elicit changes in the synaptic efficacy of neuronal circuits (Freund *et al*., 2003), the expression of CB_2 receptors in the naive brain remains controversial (Zimmer *et al*., 1999; Van Sickle *et al*., 2005; Onaivi *et al*., 2006) and the effects of endocannabinoids in the brain are usually attributed to an action at CB_1 receptors. CB_2 receptors are abundant outside the CNS and are particularly associated with immune tissues, such as spleen and thymus, as well as in various circulating immune cell populations (Klein *et al*., 2003). In our phMRI study, no significant changes in brain activity were observed in rats treated with AM1241. This is despite the fact that high brain levels are achieved at relevant doses (Table 2). This suggests that if CB_2 receptors are present in the naive brain, they are not functionally detectable using phMRI

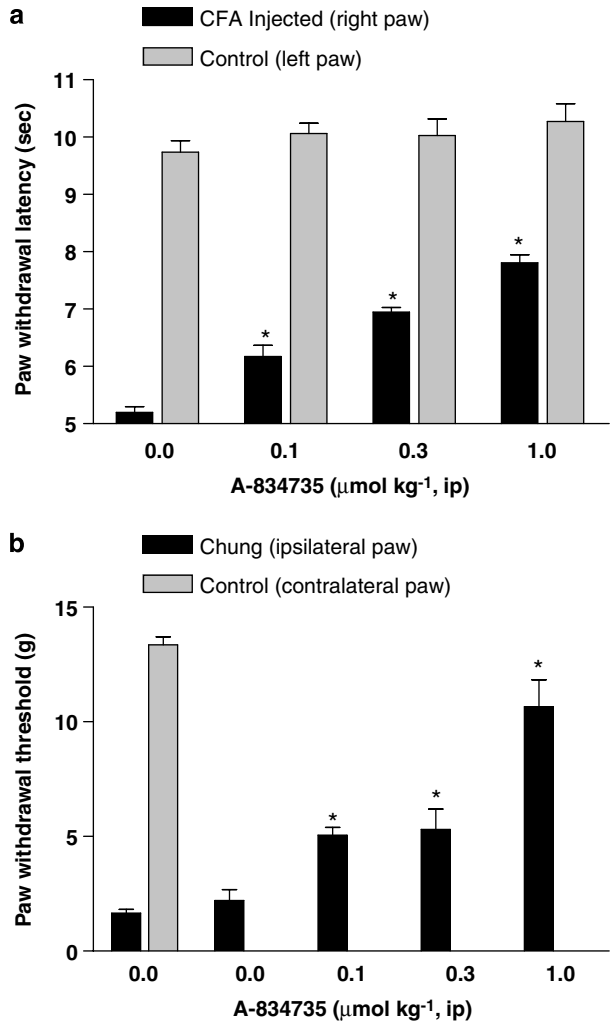

Figure 6 Effects of A-834735 (injected i.p. 30 min before testing and 48 h after CFA) on CFA-induced chronic inflammatory thermal hyperalgesia (**a**) and effects of A-834735 (injected 30 min prior to testing) on tactile allodynia in a rat neuropathic pain model of sciatic nerve chronic constriction injury (CCI). Data represent mean ± s.e. mean. *$P<0.05$, *$P<0.01$ compared to vehicle-treated rats ($n=12$ per group). A-834735 dose-dependently attenuated thermal hyperalgesia (**a**) and neuropathic pain (**b**) as reflected by increased paw withdrawal threshold and latencies, respectively.

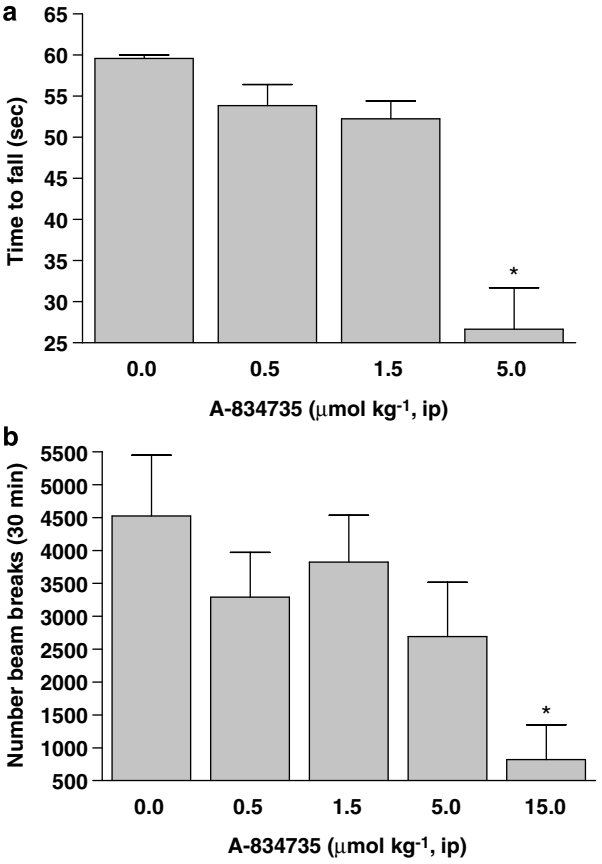

Figure 7 Effects of A-834735 (i.p.) on rotorod performance (**a**) and spontaneous horizontal locomotor activity (**b**). A-834735 impaired rotorod performance and decreased exploratory locomotor behaviour at higher doses, reaching statistical significance at the highest dose tested in each case. Data are mean ± s.e. mean, $n=7$ rats/group for rotorod and $n=8$ rats/group for locomotor activity. **$P<0.001$ vs vehicle control.

methods. Additional data with other proprietary CB_2-selective agonists also support this contention (unpublished observations). Recently, Van Sickle *et al*. (2005) demonstrated the presence of CB_2 receptor mRNA and protein localization in brainstem neurons. While some brainstem regions were included in our present imaging studies, AM1241 did not have any effect on brainstem activity. It is possible that under the current test conditions, CB_2 receptors, if proven to be present in the brain stem, are not activated by AM1241. This is in contrast to its profound efficacy observed in pain models (Malan *et al*., 2001), a finding that is consistent with the behaviour of a protean agonist at the human CB_2 receptor (Yao *et al*., 2006). Although it exhibited agonist properties at the rat CB_1 receptor in recombinant cells at high concentrations, in phMRI studies high doses of AM1241 failed to either produce an expected CB_1 activation pattern or to block functional CB_1 activation by A-834735 in animals, indicating that inconsistent pharmacology also exists for AM1241 at CB_1 receptors. The lack of brain activation by AM1241 in phMRI studies is consistent though with the report that AM1241 administration in animals did not induce psychotropic effects (Malan *et al*., 2001). However, it is not clear if the observed lack of brain activation for AM1241 is contributed by receptors that may produce a confounding effect to CB_1, as it has recently been demonstrated that μ-opioid receptors contribute to AM1241-evoked analgesia (Ibrahim *et al*., 2006). Of course, the current findings with phMRI in naive rats do not differentiate between the potential lack of CB_2 receptor expression and the presence of non-functional CB_2 receptors in regions of the brain. It is also possible that changes in neural brain activity may occur in response to treatment with CB_2 receptor agonists in rats with underlying pathology (for example, neuropathic pain), a point requiring further investigation.

The antinociceptive efficacy of cannabinoids has been demonstrated previously but discord exists with regard to the mechanisms and sites of action of such drugs (Mackie,

Table 3 Comparison of dose-related *in vivo* behavioural measures and phMRI brain activation induced by A-834735 or AM1241 in rats

Compound	*Dose (μmol kg^{-1})*	In vivo *pain models (i.p.)*		*Activity (i.p.)*	*phMRI (i.v.)*
		CFA (inflammatory pain)	*Chung (spinal nerve ligation)*	*Side effects (spontaneous locomotor)*	*Function (neural activation)*
A-834735	0.3	+ +	+ +		+
	1	+ + +	+ + + +	+	+ +
	3			+ + +	+ + +
	10				
AM1241	10	+ +		—*	
	30		+ + +		—
	100				—

phMRI, pharmacological magnetic resonance imaging.
(+ + + + > 75%; + + + 75–50%; + + 50–25%; + < 25% efficacy/effect; – no effect; blank not tested)
*3.3 mg kg^{-1} i.p. (Malan *et al.*, 2001).

2006; Pacher *et al.*, 2006). What is known, however, is that cannabinoid receptors are broadly expressed in key regions of the CNS and periphery that play important roles in modulating pain transmission, processing or perception, such as primary afferents, dorsal-horn neurons, nuclei in the brainstem, somatosensory and frontal cortices (Mackie, 2006). Studies with CB_1 and CB_2 receptor knockout mice have shown the importance of both receptor subtypes in mediating analgesia (Ledent *et al.*, 1999; Zimmer *et al.*, 1999; Ibrahim *et al.*, 2006). Interestingly, recent work proposes a peripheral site of action for cannabinoids at CB_1 receptors using conditional CB_1 receptor knockout mice (Agarwal *et al.*, 2007). These authors propose that the well-known side effects associated with central CB_1 receptor activation may be avoided by targeting peripheral CB_1 receptors with antinociceptive drugs that do not cross the blood–brain barrier. In this study, we observed changes in brain activity associated with CB_1 receptor activation by the non-selective agonist, A-834735, which readily crosses into the brain. Indeed, A-834735 increased brain activation in brain regions thought to be responsible for mediating intoxication, cognitive and memory impairments resulting from CB_1 receptor activation such as the prefrontal and cingulate cortices as well as the hippocampus. Further, brain regions important for motor coordination and function such as the cerebellum and motor cortex were also affected by A-834735 in our phMRI studies at doses consistent with the adverse effects we observed with the same drug in nonspecific spontaneous exploration and rotorod studies (Figure 7, Table 3). Thus, phMRI has the ability to determine unambiguously selectivity for CB_2 over CB_1 receptors of drugs designed to be CB_2-selective. This is critical since novel drugs may behave differently in intact *in vivo* systems compared to *in vitro* recombinant systems and important future contributions that CB_2-selective agonists may have as antinociceptive drugs can be fully explored with the confidence that CB_1-mediated adverse effects can be avoided. Finally, CB_1 receptors in the CNS have been shown to mediate stress-induced analgesia, probably through increased release of the endogenous endocannabinoids, 2-arachidonoylglycerol and anandamide (Hohmann *et al.*, 2005). In this study, animals were imaged under awake conditions and thus the possible involvement of stress cannot be excluded. However, since rimonabant alone had no effect on basal activity and pharmacological specificity was demonstrated for A-834735, the observed changes in brain activity are likely to be mediated by CB_1 receptors and not the result of stress.

In summary, our results show that functional selectivity for CB_1 vs CB_2 receptors in the naive brain can be determined non-invasively using phMRI in awake rats. Since the goal of many investigators developing novel CB_2 agonists as antinociceptive drugs is to avoid CB_1-mediated CNS adverse effects, phMRI offers a powerful tool for confirming selectivity. Our data also indicate that CB_2 receptors, if present in the naive rat brain, are not functionally detectable *in vivo* using our sensitive phMRI technique.

Acknowledgements

We wish to extend our gratitude to Drs Wolfgang Ebert, Bernd Misselwitz, and Hans Bauer (Bayer Schering Pharma AG, Berlin, Germany) for providing SH U 555 C and to Drs Jim Sullivan and Michael Decker for insightful discussion.

Conflict of interest

All authors are employees of Abbott laboratories, the source of funding for this research.

References

Agarwal N, Pacher P, Tegeder I, Amaya F, Constantin CE, Brenner GJ *et al.* (2007). Cannabinoids mediate analgesia largely via peripheral type 1 cannabinoid receptors in nociceptors. *Nat Neurosci* **10**: 870–879.

Austin VC, Blamire AM, Allers KA, Sharp T, Styles P, Matthews PM *et al.* (2005). Confounding effects of anesthesia on functional activation in rodent brain: a study of halothane and alpha-chloralose anesthesia. *NeuroImage* **24**: 92–100.

Burns HD, Van Laere K, Sanabria-Bohorquez S, Hamill TG, Bormans G, Eng WS *et al.* (2007). [18F]MK-9470, a positron emission tomography (PET) tracer for *in vivo* human PET brain imaging of the cannabinoid-1 receptor. *Proc Natl Acad Sci USA* **104**: 9800–9805.

Campbell FA, Tramer MR, Carroll D, Reynolds DJ, Moore RA, McQuay HJ (2001). Are cannabinoids an effective and safe treatment option in the management of pain? A qualitative systematic review. *BMJ* **323**: 13–16.

Chaplan SR, Bach FW, Pogrel JW, Chung JM, Yaksh TL (1994). Quantitative assessment of tactile allodynia in the rat paw. *J Neurosci Methods* **53**: 55–63.

Chen YC, Galpern WR, Brownell AL, Matthews RT, Bogdanov M, Isacson O *et al.* (1997). Detection of dopaminergic neurotransmitter activity using pharmacologic MRI: correlation with PET, microdialysis, and behavioral data. *Magn Reson Med* **38**: 389–398.

Chin CL, Pauly JR, Surber BW, Skoubis PD, McGaraughty SP, Hradil V *et al.* (2007). Pharmacological MRI in awake rats predicts selective binding of a4b2 nicotinic receptors. *Synapse* (in press).

Choi JK, Mandeville JB, Chen YI, Kim YR, Jenkins BG (2006). High resolution spatial mapping of nicotine action using pharmacologic magnetic resonance imaging. *Synapse* **60**: 152–157.

Cox RW (1996). AFNI: software for analysis and visualization of functional magnetic resonance neuroimages. *Comput Biomed Res* **29**: 162–173.

Croxford JL (2003). Therapeutic potential of cannabinoids in CNS disease. *CNS Drugs* **17**: 179–202.

Dart MJ, Frost JM, Tietje KR, Daza A, Grayson GK, Fan Y *et al.* (2006). 1-alkyl-3-keto-indoles: identification and *in vitro* characterization of a series of potent cannabinoid ligands. *International Cannabinoid Research Society*; June 25–28; Budapest, Hungary, p 125.

Dixon AL, Prior M, Morris PM, Shah YB, Joseph MH, Young AM (2005). Dopamine antagonist modulation of amphetamine response as detected using pharmacological MRI. *Neuropharmacology* **48**: 236–245.

Fox GB, McGaraughty SP, Luo Y (2006). Pharmacological and functional magnetic resonance imaging techniques in CNS Drug Discovery. *Expert Op Drug Discov* **1**: 211–224.

Freund TF, Katona I, Piomelli D (2003). Role of endogenous cannabinoids in synaptic signaling. *Physiol Rev* **83**: 1017–1066.

Gozzi A, Schwarz A, Reese T, Bertani S, Crestan V, Bifone A (2005). Region-specific effects of nicotine on brain activity: a pharmacological MRI study in the drug-naive rat. *Neuropsychopharmacology* **31**: 1690–1703.

Gutierrez T, Farthing JN, Zvonok AM, Makriyannis A, Hohmann AG (2007). Activation of peripheral cannabinoid CB1 and CB2 receptors suppresses the maintenance of inflammatory nociception: a comparative analysis. *Br J Pharmacol* **150**: 153–163.

Hargreaves K, Dubner R, Brown F, Flores C, Joris J (1988). A new and sensitive method for measuring thermal nociception in cutaneous hyperalgesia. *Pain* **32**: 77–88.

Herkenham M, Lynn AB, Little MD, Johnson MR, Melvin LS, de Costa BR *et al.* (1990). Cannabinoid receptor localization in brain. *Proc Natl Acad Sci USA* **87**: 1932–1936.

Hohmann AG, Suplita RL, Bolton NM, Neely MH, Fegley D, Mangieri R *et al.* (2005). An endocannabinoid mechanism for stress-induced analgesia. *Nature* **435**: 1108–1112.

Honey G, Bullmore E (2004). Human pharmacological MRI. *Trends Pharmacol Sci* **25**: 366–374.

Ibrahim MM, Deng H, Zvonok AM, Cockayne DA, Kwan J, Mata HP *et al.* (2003). Activation of CB_2 cannabinoid receptors by AM1241 inhibits experimental neuropathic pain: Pain inhibition by receptors not present in CNS. *Proc Natl Acad Sci USA* **100**: 10529–10533.

Ibrahim MM, Rude ML, Stagg NJ, Mata HP, Lai J, Vanderah TW *et al.* (2006). CB2 cannabinoid receptor mediation of antinociception. *Pain* **122**: 36–42.

Ireland MD, Lowe AS, Reavill C, James MF, Leslie RA, Williams SC (2005). Mapping the effects of the selective dopamine D2/D3 receptor agonist quinelorane using pharmacological magnetic resonance imaging. *Neuroscience* **133**: 315–326.

Iversen L, Chapman V (2002). Cannabinoids: a real prospect for pain relief? *Curr Opin Pharmacol* **2**: 50–55.

Jones N, O'Neill MJ, Tricklebank M, Libri V, Williams SC (2005). Examining the neural targets of the AMPA receptor potentiator LY404187 in the rat brain using pharmacological magnetic resonance imaging. *Psychopharmacology (Berl)* **180**: 743–751.

Kim SH, Chung JM (1992). An experimental model for peripheral neuropathy produced by segmental spinal nerve ligation in the rat. *Pain* **50**: 355–363.

King JA, Garelick TS, Brevard ME, Chen W, Messenger TL, Duong TQ *et al.* (2006). Procedure for minimizing stress for fMRI studies in conscious rats. *J Neurosci Methods* **148**: 154–160.

Klein TW, Newton C, Larsen K, Lu L, Perkins I, Nong L *et al.* (2003). The cannabinoid system and immune modulation. *J Leukoc Biol* **74**: 486–496.

Ledent C, Valverde O, Cossu G, Petitet F, Aubert JF, Beslot F *et al.* (1999). Unresponsiveness to cannabinoids and reduced addictive effects of opiates in CB1 receptor knockout mice. *Science* **283**: 401–404.

Leslie RA, James MF (2000). Pharmacological magnetic resonance imaging: a new application for functional MRI. *Trends Pharmacol Sci* **21**: 314–318.

Mackie K (2006). Cannabinoid receptors as therapeutic targets. *Annu Rev Pharmacol Toxicol* **46**: 101–122.

Malan Jr TP, Ibrahim MM, Deng H, Liu Q, Mata HP, Vanderah T *et al.* (2001). CB2 cannabinoid receptor-mediated peripheral antinociception. *Pain* **93**: 239–245.

Malan Jr TP, Ibrahim MM, Deng H, Liu Q, Mata HP, Vanderah TW *et al.* (1998). CB2C annabinoid receptor-mediated peripheral antinociception. *Pain* **93**: 239–245.

Malan Jr TP, Ibrahim MM, Lai J, Vanderah TW, Makriyannis A, Porreca F (2003). CB2 cannabinoid receptor agonists: pain relief without psychoactive effects? *Curr Opin Pharmacol* **3**: 62–67.

Mandeville JB, Marota JJ, Kosofsky BE, Keltner JR, Weissleder R, Rosen BR *et al.* (1998). Dynamic functional imaging of relative cerebral blood volume during rat forepaw stimulation. *Magn Reson Med* **39**: 615–624.

Mukherjee S, Adams M, Whiteaker K, Daza A, Kage K, Cassar S *et al.* (2004). Species comparison and pharmacological characterization of rat and human CB2 cannabinoid receptors. *Eur J Pharmacol* **505**: 1–9.

Onaivi ES, Ishiguro H, Gong JP, Patel S, Perchuk A, Meozzi PA *et al.* (2006). Discovery of the presence and functional expression of cannabinoid CB_2 receptors in brain. *Ann N Y Acad Sci* **1074**: 514–536.

Pacher P, Batkai S, Kunos G (2006). The endocannabinoid system as an emerging target of pharmacotherapy. *Pharmacol Rev* **58**: 389–462.

Paxinos G, Watson C (1998). *The Rat Brain in Stereotaxic Coordinates*. Academic Press: San Diego.

Pertwee RG (2006). The pharmacology of cannabinoid receptors and their ligands: an overview. *Int J Obes (Lond)* **30**: S13–S18.

Reese T, Bjelke B, Porszasz R, Baumann D, Bochelen D, Sauter A *et al.* (2000). Regional brain activation by bicuculline visualized by functional magnetic resonance imaging. Time-resolved assessment of bicuculline-induced changes in local cerebral blood volume using an intravascular contrast agent. *NMR Biomed* **13**: 43–49.

Richardson JD, Kilo S, Hargreaves KM (1998). Cannabinoids reduce hyperalgesia and inflammation via interaction with peripheral CB1 receptors. *Pain* **75**: 111–119.

Schwarz A, Gozzi A, Reese T, Bertani S, Crestan V, Hagan J *et al.* (2004). Selective dopamine D(3) receptor antagonist SB-277011-A potentiates phMRI response to acute amphetamine challenge in the rat brain. *Synapse* **54**: 1–10.

Shah YB, Prior MJ, Dixon AL, Morris PG, Marsden CA (2004). Detection of cannabinoid agonist evoked increase in BOLD contrast in rats using functional magnetic resonance imaging. *Neuropharmacology* **46**: 379–387.

Skoubis PD, Hradil V, Chin CL, Luo Y, Fox GB, McGaraughty S (2006). Mapping brain activity following administration of a nicotinic acetylcholine receptor agonist, ABT-594, using functional magnetic resonance imaging in awake rats. *Neuroscience* **137**: 583–591.

Tombach B, Reimer P, Bremer C, Allkemper T, Engelhardt M, Mahler M *et al.* (2004). First-pass and equilibrium-MRA of the aortoiliac region with a superparamagnetic iron oxide blood pool MR contrast agent (SH U 555 C): results of a human pilot study. *NMR Biomed* **17**: 500–506.

Van Sickle MD, Duncan M, Kingsley PJ, Mouihate A, Urbani P, Mackie K *et al.* (2005). Identification and functional

characterization of brainstem cannabinoid CB2 receptors. *Science* **310**: 329–332.

Wise RG, Tracey I (2006). The role of fMRI in drug discovery. *J Magn Reson Imaging* **23**: 862–876.

Xi ZX, Wu G, Stein EA, Li SJ (2002). GABAergic mechanisms of heroin-induced brain activation assessed with functional MRI. *Magn Reson Med* **48**: 838–843.

Yao BB, Mukherjee S, Fan Y, Garrison TR, Daza AV, Grayson GK *et al.* (2006). In vitro pharmacological characterization of AM1241: a protean agonist at the cannabinoid CB2 receptor? *Br J Pharmacol* **149**: 145–154.

Zhang Z, Andersen AH, Avison MJ, Gerhardt GA, Gash DM (2000). Functional MRI of apomorphine activation of the basal ganglia in awake rhesus monkeys. *Brain Res* **852**: 290–296.

Zimmer A, Zimmer AM, Hohmann AG, Herkenham M, Bonner TI (1999). Increased mortality, hypoactivity, and hypoalgesia in cannabinoid CB1 receptor knockout mice. *Proc Natl Acad Sci USA* **96**: 5780–5785.